

Production of $\omega\pi^0$ pairs in electron-positron annihilation

A. B. Arbuzov

*Bogoliubov Laboratory of Theoretical Physics, JINR, Dubna, 141980 Russia and
Department of Higher Mathematics, University Dubna, Dubna, 141980 Russia*

E. A. Kuraev and M. K. Volkov

Bogoliubov Laboratory of Theoretical Physics, JINR, Dubna, 141980 Russia

(Received 27 December 2010; revised manuscript received 11 March 2011; published 21 April 2011)

The process of electron-positron annihilation into a pair of π^0 and ω mesons is considered in the framework of the $SU(2)\times SU(2)$ Nambu–Jona-Lasinio model. Contributions of intermediate photons, $\rho(770)$ and $\rho'(1450)$ vector mesons are taken into account. It is shown that the bulk of the cross section at energies below 2 GeV is provided by the process with intermediate $\rho'(1450)$ state. The contribution due to single photon and $\rho(770)$ exchange is in agreement with the vector meson dominance model. Numerical results are compared with experimental data.

DOI: [10.1103/PhysRevC.83.048201](https://doi.org/10.1103/PhysRevC.83.048201)

PACS number(s): 12.39.Fe, 13.66.Bc, 13.20.Jf

I. INTRODUCTION

Studies of the process of associated production of π^0 and ω mesons at colliding electron-positron beams provide interesting information about meson interactions at low energies. Moreover, this channel is one of the contributions to the total cross section of e^+e^- annihilation into hadrons, which is required for a precise determination of the hadronic vacuum polarization.

The annihilation into the $\omega\pi^0$ pair at energies below 2 GeV was studied experimentally at DM2 [1], ND [2], SND [3], and CMD-2 [4]. The same interactions can be also found in the tau lepton decay $\tau \rightarrow \pi\omega\nu_\tau$ studied at CLEO II [5].

For a theoretical description of the process under consideration, the vector-dominance-like models were used (see, e.g., Ref. [4]). To fit the experimental data, a set of additional parameters describing contributions of amplitudes with virtual $\rho(770)$, $\rho'(1450)$, and $\rho''(1700)$ mesons was introduced. The energy dependence of these parameters was neglected. Earlier, the process of $\rho' \rightarrow \omega\pi$ decay was considered within a relativistically generalized quark model in Ref. [6] and in a nonrelativistic quark model [7]. In Ref. [8], the reaction $e^+e^- \rightarrow \omega\pi^0$ was considered in the vicinity of the ϕ meson mass region, where the KLOE experimental data are available [9]. In this paper, we will not work specially at this resonance, so the region from the threshold up to about 2 GeV c.m.s. energy will be considered without taking into account the ϕ meson contribution. Recently, in Ref. [10], the process was considered in frames of a nonrelativistic quark model. It is argued there that the process at energies below 2 GeV is dominated by the two-step process in which the primary quark-antiquark pair forms a ρ meson in the ground or excited state and then the vector meson decays into ω and π . It is important to note that the studies in Refs. [4,5,10] concluded that the contribution of the $\rho''(1700)$ to the process is small. Following the results, this paper will neglect the contribution of the amplitude with intermediate $\rho''(1700)$ meson. Meanwhile, in Ref. [11], it is claimed that, for a simultaneous description of a series of different annihilation and decay processes, all three rho meson states should be taken into account.

In this paper, we will use the version of the Nambu–Jona-Lasinio (NJL) model, which allows us to describe both the ground and the first radial-excited meson states [12–16], for the description of the process $e^+e^- \rightarrow \omega\pi^0$. Note that, for the description of the amplitudes with virtual photon and the ground $\rho(770)$ state, one can use the standard NJL model [17–24]. It is worth noting that, for the case of the ground meson states, both versions of the NJL model lead to the same results (see, e.g., Refs. [14,25]). In our model, it is possible to describe as the transition amplitudes $\gamma^* \rightarrow \rho, \rho'$ as well as the vertexes $\gamma^*, \rho, \rho' \rightarrow \pi^0\omega$ without introduction of any additional arbitrary parameters. Moreover, the description of the vertexes using the quark triangle diagram of the anomaly type allows us to get their energy dependence.

II. PROCESS AMPLITUDES

For the description of the first two diagrams (see Figs. 1 and 2), we need the part of the standard NJL Lagrangian that describes interactions of photons, pions, and vector ρ and ω mesons with quarks (see Refs. [17,21,22]). It has the form

$$\Delta\mathcal{L}_1 = \bar{q} \left[i\hat{\partial} - m + eQ\hat{A} + ig_\pi\gamma_5\tau_3\pi^0 + \frac{g_\rho}{2}\gamma_\mu(I\hat{\omega} + \tau_3\hat{\rho}^0) \right] q, \quad (1)$$

where $\bar{q} = (\bar{u}, \bar{d})$ with u and d quark fields; $m = \text{diag}(m_u, m_d)$, $m_u = m_d = 280$ MeV is the constituent quark mass; $Q = \text{diag}(2/3, -1/3)$ is the electromagnetic quark charge matrix; e is the electron charge; A , π^0 , ω , and ρ^0 are the photon, pion, ω , and ρ meson fields, respectively; g_π is the pion coupling constant $g_\pi = m_u/f_\pi$, where $f_\pi = 93$ MeV is the pion decay constant; g_ρ is the vector meson coupling constant $g_\rho \approx 6.14$ corresponding to the standard relation $g_\rho^2/(4\pi) = 3$; $I = \text{diag}(1, 1)$; and τ_3 is the third Pauli matrix.

All three amplitudes contain the common part corresponding to the $e^+e^- \gamma$ vertex and the photon propagator. So, the

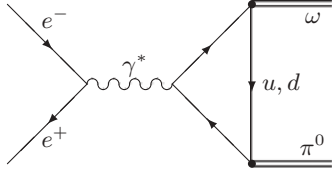


FIG. 1. The Feynman diagram with photon exchange.

sum of the amplitudes can be cast in the form

$$T^\lambda = \bar{e}\gamma_\mu e \frac{1}{s} \{T_1^{\mu\lambda} + T_2^{\mu\lambda} + T_3^{\mu\lambda}\} \varepsilon_\lambda(\omega), \quad (2)$$

where $s = [p_1(e^+) + p_2(e^-)]^2 \equiv q^2$. The first part T_1 is just the triangle quark diagram of the anomaly type. Note that the loop integral in it is finite. Following Refs. [25–27], we use here the naive confinement approach and neglect the imaginary part of the loop integral.

The integral over the energy k^0 of the virtual loop momentum is calculated analytically using the residue method. The integral over \vec{k} is taken numerically. Even though this integral is convergent, we set the cutoff for the upper value of $|\vec{k}|$ equal to $\Lambda = 1.03$ GeV [28]. This cutoff will be necessary in contributions of the radially excited meson states. Here, the cutoff is applied for homogeneity of the approach. The numerical result for the convergent integral does not change considerably if the cutoff were to be removed. The imaginary part is neglected by taking the principal value of the integral.

The second contribution T_2 contains three factors. The first one is the transition of the photon into the ρ meson, which is described in Ref. [17]:

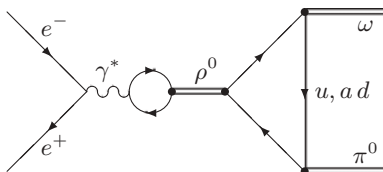
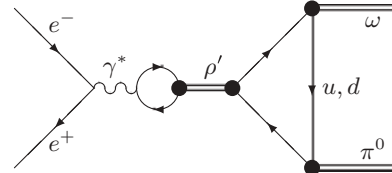
$$\frac{e}{g_\rho} (g^{vv'} q^2 - q^v q^{v'}). \quad (3)$$

Note that, contrary to the case of the triangle diagram, the quark loop describing the γ - ρ transition contains a logarithmic divergence. The standard NJL methods were applied for its regularization using the cutoff value. The second factor is the ρ meson propagator

$$\frac{i g^{v'v''}}{q^2 - M_\rho^2 + i M_\rho \Gamma_\rho}, \quad (4)$$

where the neutral ρ meson mass $M_\rho = 775$ MeV and width $\Gamma_\rho = 146$ MeV [29]. Note that the nondiagonal terms in the numerator of the vector particle propagator were dropped because of the gradient invariance of the triangle diagram. The third factor is the same triangle diagram as in the first amplitude T_1 .

A more complicated situation appears for the third contributions T_3 (see Fig. 3) because we deal here with the radially excited ρ' meson. Instead of the Lagrangian (1), we

FIG. 2. The Feynman diagram with ρ meson exchange.FIG. 3. The Feynman diagram with ρ' meson exchange.

use here an extended version of the NJL Lagrangian, which allows us to describe both ground and radial-excited meson states [13,14,25]:

$$\Delta\mathcal{L}_2 = \bar{q}(k') \{i\hat{\partial} - m + eQ\hat{A} + A_\pi \tau^3 \gamma_5 \pi^0(p) + A_\omega \hat{\omega}(p) - A_{\rho'} \tau^3 \hat{\rho}'(p)\} q(k), \quad p = k - k' \quad (5)$$

$$A_\pi = g_{\pi_1} \frac{\sin(\alpha + \alpha_0)}{\sin(2\alpha_0)} + g_{\pi_2} f(k^\perp{}^2) \frac{\sin(\alpha - \alpha_0)}{\sin(2\alpha_0)},$$

$$A_\omega = g_{\rho_1} \frac{\sin(\beta + \beta_0)}{\sin(2\beta_0)} + g_{\rho_2} f(k^\perp{}^2) \frac{\sin(\beta - \beta_0)}{\sin(2\beta_0)},$$

$$A_{\rho'} = g_{\rho_1} \frac{\cos(\beta + \beta_0)}{\sin(2\beta_0)} + g_{\rho_2} f(k^\perp{}^2) \frac{\cos(\beta - \beta_0)}{\sin(2\beta_0)}.$$

The radially excited states were introduced in the NJL model with the help of the form factor in the quark-meson interaction

$$f(k^\perp{}^2) = (1 - d|k^\perp{}^2|) \Theta(\Lambda^2 - |k^\perp{}^2|),$$

$$k^\perp = k - \frac{(kp)p}{p^2}, \quad d = 1.78 \text{ GeV}^{-2} \quad (6)$$

where k and p are the quark and meson momenta, respectively. The filled circles in Fig. 3 denote the presence of the form factor in the quark-meson vertexes. Note that the NJL model itself and its extended version can be used only for sufficiently low energies. In this paper, we attempt to receive qualitative results working at energies up to 2 GeV.

Coupling constants g_{π_1} and g_{ρ_1} coincide with g_π and g_ρ constants introduced above in the standard NJL version. The other coupling constants are defined via one-loop integrals

$$g_{\pi_2} = [4I_2^{f^2}]^{-1/2}, \quad g_{\rho_2} = [\frac{2}{3}I_2^{f^2}]^{-1/2} = \sqrt{6}g_{\pi_2}, \quad (7)$$

where

$$I_m^{f^n} = -iN_c \int \frac{d^4k}{(2\pi)^4} \frac{[f(k^\perp{}^2)]^n}{(m^2 - k^2)^m}, \quad n, m = 1, 2.$$

The angles $\alpha_0 = 59.06^\circ$, $\alpha = 59.38^\circ$, $\beta_0 = 61.53^\circ$, and $\beta = 76.78^\circ$ were defined in Refs. [14,25] to describe mixing of the ground and excited meson states. This contribution T_3 again consists of three parts. The γ - ρ_2 transition (the γ - ρ_1 transition coincides with the standard γ - ρ one) can be expressed via the γ - ρ transition (3) with the additional factor [13,14]

$$\Gamma = \frac{I_2^f}{\sqrt{I_2 I_2^{f^2}}} \approx 0.47. \quad (8)$$

So, the γ - ρ' transition takes the form

$$\frac{e}{g_\rho} (g^{vv'} q^2 - q^v q^{v'}) \left\{ \frac{\sin(\beta + \beta_0)}{\sin(2\beta_0)} + \Gamma \frac{\sin(\beta - \beta_0)}{\sin(2\beta_0)} \right\}.$$

We take the ρ' propagator taken in the Breit-Wigner form

$$\frac{g^{v'v''}}{q^2 - M_{\rho'}^2 + i\sqrt{q^2}\Gamma_{\rho'}(q^2)}, \quad (9)$$

where the running ρ' width reads as

$$\begin{aligned} \Gamma_{\rho'}(q^2) = & \Gamma(\rho' \rightarrow 2\pi) + \Gamma(\rho' \rightarrow \omega\pi^0) + [\Gamma_{\rho'}(M_{\rho'}) \\ & - \Gamma(\rho' \rightarrow \omega\pi^0) - \Gamma(\rho' \rightarrow \omega\pi^0)] \\ & \times \Theta(\sqrt{s} - M_{a_1} + M_{\pi}) \times \left(\frac{p_{a_1}(s)}{p_{a_1}(M_{\rho'})} \right), \quad (10) \end{aligned}$$

where $p_{a_1}(s)$ is the momentum of the a_1 meson in the decay $\rho' \rightarrow a_1\pi$. We assume that, below the threshold of the reaction $\rho' \rightarrow a_1\pi$, the main contribution of the width is given by the two channels $\rho' \rightarrow 2\pi$ and $\rho' \rightarrow \omega\pi^0$. Above the peak $\sqrt{s} \geq M_{\rho'}$, where many other channels are opened, we use the complete width $\Gamma_{\rho'} = 340$ MeV (we take the value at the lower PDG [29] boundary). The transition to the complete width is approximately described by the linear switching of the contribution due to the decay $\rho' \rightarrow a_1\pi$ being one of the most probable channels. The values $\Gamma(\rho' \rightarrow 2\pi) = 22$ MeV and $\Gamma(\rho' \rightarrow \omega\pi^0) = 75$ MeV were calculated in [14] in agreement with the experimental data [30]. Since we are working close to the $\omega\pi$ threshold, taking into account the running width is important. Running of the ρ meson width is less important numerically, since the ρ meson contribution is relatively small.

III. NUMERICAL RESULTS AND DISCUSSION

Now we can estimate the contributions of the considered amplitudes into the total process cross section. The details of phase volume calculations and evaluation of the cross section can be found in Ref. [27]. For our case, it takes the form

$$\begin{aligned} \sigma(s) = & \frac{3\alpha^2}{32\pi^3 s^3} \lambda^{3/2}(s, M_{\omega}^2, M_{\pi}^2) \frac{g_{\rho}^2}{f_{\pi}^2} |J^{(3)}|^2 \\ & \times Br(\omega \rightarrow \pi^0\gamma), \\ \lambda(s, M_{\omega}^2, M_{\pi}^2) = & (s - M_{\omega}^2 - M_{\pi}^2)^2 - 4M_{\omega}^2 M_{\pi}^2, \quad (11) \end{aligned}$$

where

$$\begin{aligned} J^{(3)} = & \left(1 - \frac{q^2}{q^2 - M_{\rho}^2 + iM_{\rho}\Gamma_{\rho}} \right) I_{\gamma}^{(3)} \\ & + \frac{\Gamma q^2}{q^2 - M_{\rho'}^2 + i\sqrt{q^2}\Gamma_{\rho'}(q^2)} I_{\rho'}^{(3)} \quad (12) \end{aligned}$$

and

$$\begin{aligned} I_{\gamma}^{(3)} \left(\frac{m^2}{s} \right) = & \int \frac{d^4k}{i\pi^2} \frac{m^2 \Theta(\Lambda^2 - |k^{\perp 2}|)}{(k^2 - m^2 + i0)} \\ & \times \frac{1}{[(k - P_{\omega})^2 - m^2 + i0][(q - k)^2 - m^2 + i0]}. \end{aligned}$$

In the first line of Eq. (12), we have the sum of the photon and rho meson exchange contributions. Their sum takes the form that coincides with the one received in the vector meson dominance model (see, e.g., [4]). In fact, the standard NJL model contains the vector dominance model [17,31,32].

Note that keeping the cutoff for the convergent integral in $I_{\gamma}^{(3)}$ entering T_1 and T_2 in Eq. (2) is not necessary, but it does not affect much the numerical result. Expression for the integral $I_{\rho'}^{(3)}$ has a rather cumbersome form and contains a combination of terms with different powers of the form factor (up to the third power). It is constructed according to the Feynman rules coming from the Lagrangian (5). For calculation of the relevant quark loop integrals, we use the method described in Ref. [25]. It is worth noting that, in our calculations, the signs of $I_{\gamma}^{(3)}$ and $I_{\rho'}^{(3)}$ appeared to be opposite in accordance with the fit to experimental data performed in [4].

The coupling constants $g_{\rho} = 6$ and $f_{\pi} = 93$ MeV in Eq. (11) are universal input parameters for the NJL model. In Ref. [4], another value for this constant was used: $f_{\rho} \approx 5$ received from the decay width $\Gamma(\rho \rightarrow e^+e^-)$. Another difference comes from the value for the coupling constant in the vertex $\rho\omega\pi$. In our model, it is $g_{\rho\omega\pi} = 3g_{\rho}^2/(8\pi^2 f_{\pi}) \approx 14.7$ GeV⁻¹, while in Ref. [4], the value $g_{\rho\omega\pi} \approx 17$ GeV⁻¹ is taken as a fitting parameter.

Figure 4 shows the experimental data [1,3,4] and the corresponding theoretical prediction (the solid line) received within the NJL phenomenological model applied here. The dashed-dotted line shows the sum of the photon and rho meson exchange contributions. The short dashed-dotted line corresponds to the pure ρ' meson exchange. The photon and ρ meson exchange is important for the threshold region, while the ρ' contribution dominates in the region $\sqrt{s} \sim M_{\rho'}$. Note that the NJL model is adjusted for applications at low energies up to about 2 GeV. In this energy range, the model gives a qualitative description of meson properties and interactions. The advantage is that the set of parameters is limited and fixed. Note that to describe the given process, we did not introduce any new parameter in the model. Presumably, adding the $\rho''(1700)$ meson contribution might improve the agreement with the experimental data above the peak, but, for the time being, the NJL model is not suited to include the second radial excitations of mesons with large masses. A more accurate description of the threshold behavior requires going beyond the Hartree-Fock approximation that was used here. Indeed,

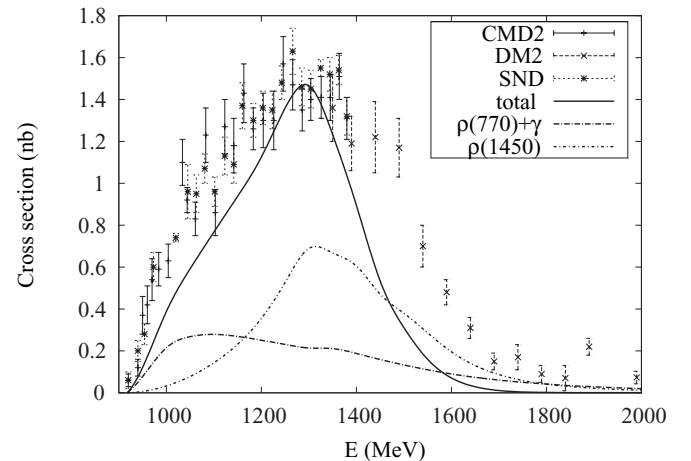


FIG. 4. Comparison of experimental results for $e^+e^- \rightarrow \pi^0\omega \rightarrow \pi^0\pi^0\gamma$ with the NJL model prediction (lines).

meson-meson final-state interactions can play an important role in the threshold domain.

The same approach was successfully applied in Refs. [14–16] for a description of mass spectra and strong decays with participation of excited mesons. In this work, we continue the work started in Refs. [25,33] devoted to description of radiative decays with participation of radially excited mesons and pass to the description of annihilation processes studied at modern e^+e^- colliders. A similar mechanism

appears in the processes of e^+e^- annihilation into, e.g., $\pi^0\gamma$, $\pi'\gamma$, and $\pi'^{\pm}\pi^{\mp}$, which will be considered elsewhere.

ACKNOWLEDGMENTS

We are grateful to A. Akhmedov, S. Gerasimov, and G. Fedotovitch for useful discussions. This work was supported by RFBR Grant No. 10-02-01295-a.

-
- [1] D. Bisello *et al.* (DM2 Collaboration), *Nucl. Phys. B, Proc. Suppl.* **21**, 111 (1991).
- [2] S. I. Dolinsky *et al.*, *Phys. Rep.* **202**, 99 (1991).
- [3] M. N. Achasov *et al.*, *Phys. Lett. B* **486**, 29 (2000).
- [4] R. R. Akhmetshin *et al.* (CMD-2 Collaboration), *Phys. Lett. B* **562**, 173 (2003).
- [5] K. W. Edwards *et al.* (CLEO Collaboration), *Phys. Rev. D* **61**, 072003 (2000).
- [6] S. B. Gerasimov and A. B. Govorkov, *Z. Phys. C: Part. Fields* **13**, 43 (1982).
- [7] F. E. Close, A. Donnachie, and Yu. S. Kalashnikova, *Phys. Rev. D* **65**, 092003 (2002).
- [8] G. Li, Y. J. Zhang, and Q. Zhao, *J. Phys. G: Nucl. Part. Phys.* **36**, 085008 (2009).
- [9] F. Ambrosino *et al.* (KLOE Collaboration), *Phys. Lett. B* **669**, 223 (2008).
- [10] K. Kittimanapun, K. Khosonthongkee, C. Kobdaj, P. Suebka, and Y. Yan, *Phys. Rev. C* **79**, 025201 (2009).
- [11] N. N. Achasov and A. A. Kozhevnikov, *Phys. Rev. D* **55**, 2663 (1997).
- [12] M. K. Volkov and C. Weiss, *Phys. Rev. D* **56**, 221 (1997).
- [13] M. K. Volkov, *Yad. Fiz.* **60**, 1094 (1997) [*Phys. At. Nucl.* **60**, 1920 (1997)].
- [14] M. K. Volkov, D. Ebert, and M. Nagy, *Int. J. Mod. Phys. A* **13**, 5443 (1998).
- [15] M. K. Volkov and V. L. Yudichev, *Fiz. Elem. Chast. Atom. Yadra* **31**, 576 (2000) [*Phys. Part. Nuclei* **31**, 282 (2000)].
- [16] M. K. Volkov and V. L. Yudichev, *Eur. Phys. J. A* **10**, 223 (2001).
- [17] M. K. Volkov, *Fiz. Elem. Chastits At. Yadra* **17**, 433 (1986) [*Sov. J. Part. Nuclei* **17**, 186 (1986)].
- [18] D. Ebert and H. Reinhardt, *Nucl. Phys. B* **271**, 188 (1986).
- [19] U. Vogl and W. Weise, *Prog. Part. Nucl. Phys.* **27**, 195 (1991).
- [20] S. P. Klevansky, *Rev. Mod. Phys.* **64**, 649 (1992).
- [21] M. K. Volkov, *Fiz. Elem. Chast. Atom. Yadra* **24**, 81 (1993) [*Phys. Part. Nuclei* **24**, 35 (1993)].
- [22] D. Ebert, H. Reinhardt, and M. K. Volkov, *Prog. Part. Nucl. Phys.* **33**, 1 (1994).
- [23] T. Hatsuda and T. Kunihiro, *Phys. Rep.* **247**, 221 (1994).
- [24] M. K. Volkov and A. E. Radzhabov, *Usp. Fiz. Nauk* **176**, 569 (2006) [*Phys.-Usp.* **49**, 551 (2006)].
- [25] E. A. Kuraev, M. K. Volkov, and A. B. Arbuzov, *Phys. Rev. C* **82**, 068201 (2010).
- [26] Yu. M. Bystritskiy, M. K. Volkov, E. A. Kuraev, E. Bartos, and M. Secansky, *Phys. Rev. D* **77**, 054008 (2008).
- [27] Yu. M. Bystritskiy *et al.*, *Int. J. Mod. Phys. A* **24**, 2629 (2009).
- [28] D. Ebert, Yu. L. Kalinovsky, L. Munchow, and M. K. Volkov, *Int. J. Mod. Phys. A* **8**, 1295 (1993).
- [29] K. Nakamura *et al.* (Particle Data Group), *J. Phys. G: Nucl. Part. Phys.* **37**, 075021 (2010).
- [30] A. B. Clegg and A. Donnachie, *Z. Phys. C: Part. Fields* **62**, 455 (1994).
- [31] M. K. Volkov and D. Ebert, *Yad. Fiz.* **36**, 1265 (1982) [*Sov. J. Nucl. Phys.* **36**, 736 (1982)].
- [32] D. Ebert and M. K. Volkov, *Z. Phys. C: Part. Fields* **16**, 205 (1983).
- [33] E. A. Kuraev and M. K. Volkov, *Phys. Lett. B* **682**, 212 (2009).